

EXPERIMENTAL ANALYSIS OF HIGH WEBER NUMBER DROP IMPACT ONTO SUPER-HYDROPHOBIC AND HYDROPHOBIC SURFACES

F. Villa¹, C. Antonini^{1,2}, I.V. Roisman², M. Marengo^{1,4}

¹ Department of Engineering, University of Bergamo, viale Marconi 5, I-24044 Dalmine (BG), Italy.

² Laboratory of Thermodynamics in Emerging Technologies, Mechanical and Process
Engineering Department, ETH Zurich, 8092 Zürich, Switzerland

³ Technische Universität Darmstadt, Alarich-Weiss-Straße 10, 64287 Darmstadt, Germany

⁴ School of Computing, Engineering and Mathematics, University of Brighton, Brighton BN2 4GJ, UK

ABSTRACT

The present work is focused on the water drop impact at high impact Weber numbers (up to $We=1100$) on surfaces with a good (hydrophobic, $100^\circ < \theta_r < 120^\circ$) or extremely high (super-hydrophobic, $\theta_r > 135^\circ$ and $\Delta\theta < 10^\circ$) water repellency. The low wettability has a potential of being an effective parameter in the heat transfer mechanism, especially in cases of two-phase flow heat transfer, and to prevent adhesion of dirt. An Air Flow Accelerated Drop generator is used to investigate the phenomena at high impact Weber numbers. The impacts are recorded to evaluate the outcome of the impact and to study various characteristics of the drop-wall interaction. Drop impacts are studied to evaluate the effect of higher impact velocity on rebound time. It is found that the impact velocity does not have an influence on rebound time. The average rebound time at different impact velocities for the lowest drop diameter ($D = 0.98$ mm) ranges from 2 ms to 4 ms, as a function of the tested surfaces. Then the effect of different drop diameters ($D = 0.98$ -1.78 mm), at fixed impact velocity, is studied. The rebound time increases when the diameter of the impacting drops increases. The tested super-hydrophobic surfaces (SHS) do not show any upper limit of rebound in the investigated range (up to $We = 1100$), i.e. the rebound is still occurring at the highest impact velocities, while for the hydrophobic surfaces an upper velocity limit exists, but only in a probabilistic manner, i.e. at a given velocity only for a percentage of the impacts a rebound occurs.

KEYWORDS: Computational methods, Heat exchanger, Cooling turbine blade, Film cooling, High temperature, Nano / Micro, Heat transfer enhancement.

1. INTRODUCTION

The fluid dynamics of a water drop impact onto a solid surface is of significant importance in a variety of industrial applications including combustible fuel injection in engines, surface cooling by liquid sprays, ink-jet printing and atomization of liquids. The reviews of drop impact phenomenon by [1] provide salient details associated with the impact process. The drop impact phenomenon comprises of several sub-processes dominantly identified as spreading, receding, splashing, and rebound [2]. An exhaustive classification of the possible outcomes resulting from a drop impacting onto a dry solid surface was carried out by [3]. Water drop impact studies are needed to investigate the mechanisms of drop rebound, to identify which are the controlling parameters for rebound (in terms of both surface wettability properties and fluid dynamics parameters). Wettability is an essential property of solid materials, which is determined by the surface geometry (the surface roughness) and the surface chemistry [4]. The surface roughness plays an important role in determining the wetting behaviour of solid surfaces. Early studies on the role of surface roughness on the drop impact process were restricted to the description of the relationship between the surface roughness and the outcome of the impact. A recent investigation of drop impacts onto dry solid surfaces under negligible ambient pressures [5] shows that surface irregularities are responsible for the droplet splashing

*Corresponding Author: marco.marengo@unibg.it

seen on rough target surfaces. The enhancement of droplet splashing with increasing surface roughness has been also noticed in several other investigations [6],[7]. Understanding wetting on rough surfaces is essential for designing and controlling wetting processes [8]. However, in addition to roughness, also the dynamic modification of the wetting properties on surfaces is still a challenging issue. The wettability of a surface is usually characterized by the contact angles. For the deposition-rebound tests, three contact angle values are important: the advancing contact angle θ_a , the receding contact angle θ_r and the contact angle hysteresis $\Delta\theta$. These angles are evaluated by the “sessile drop method”. A drop of liquid is formed on the tip of the needle attached to a syringe and the contact angle is measured with high-resolution cameras and appropriate software to capture and analyze the image. The largest possible contact angle, without increasing its solid/liquid interfacial area that is measured by adding volume dynamically, is the advancing angle, θ_A . Volume is then removed to produce the smallest possible angle, the receding angle, θ_r . The difference between the advancing and receding angle is the contact angle hysteresis ($\Delta\theta$). Fig 1 depicts a typical sequence of images used for this evaluation.

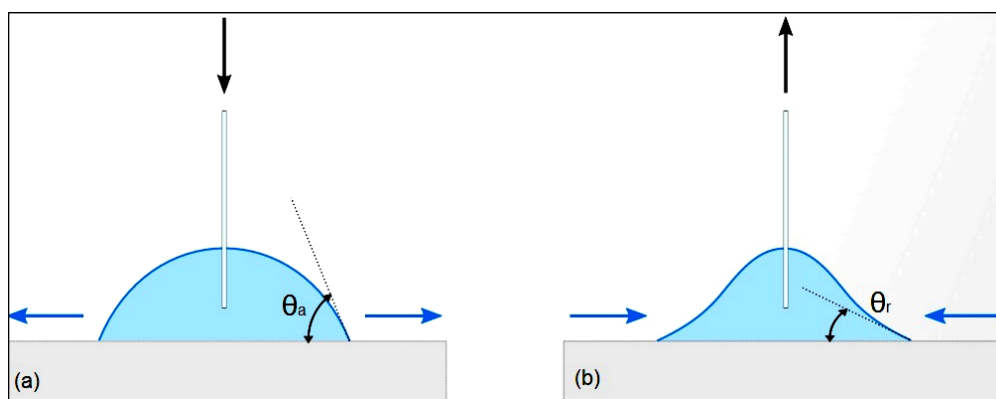


Fig 1: Sessile drop test to evaluate advancing and receding contact angles.

Surfaces with high water repellency (hydrophobic surfaces) or with very high water repellency (super-hydrophobic surfaces) are usually obtained by mixing chemistry and surface topology [9]. Smooth surfaces of low-energy-materials typically provide a maximum advancing contact angle of 120° . However, a lotus leaf demonstrates water contact angles as high as 160° , due to its special surface structure [4].

The attention of this work is focused on the drop impacts on surfaces with a good (hydrophobic) or extremely high (super-hydrophobic) water repellency. In a previous work [10] the role of the receding contact angle was investigated and proven to be the principal wetting parameter to define the drop rebound outcome. It was found that on hydrophilic surfaces ($\theta_r < 100^\circ$) rebound never occurs and the drop remains on the surface. On hydrophobic surfaces ($100^\circ < \theta_r < 120^\circ$), drops deposit gently up to a minimum Weber number (10-20), while the rebound occurs for Weber numbers in the range 20-585. Complete rebound can be observed for the super-hydrophobic surfaces ($\theta_r > 135^\circ$). The transition from a Cassie-Baxter to Wenzel state [11],[9], usually invoked in order to explain why a drop remains stuck on the super-hydrophobic surfaces, does not occur for the tested super-hydrophobic surfaces in the range of Weber number 20-585. To investigate the behaviour of impacts with a Weber number higher than about 600 it is necessary to increase the velocity of the impact. In [12] drop impact at very high velocity (from 10 to 40 m/s) were used to study the rupture of thin water films spreading radially outward on a solid surface by photographs of water droplets impacting, to determine conditions under which a radially spreading water film, created by the normal impact of a circular liquid jet on a horizontal surface, would either rupture or remain stable. In the present investigation the drop impact test at high weber number evaluates not only the outcome of the impact (deposition or rebound) but also the rebound time, when rebound occur, and the maximum spreading. These parameters are compared with correlation found in the literature [13],[14].

2. MATERIALS

Five different surfaces are used in the experiments. The selected surfaces can be divided into one hydrophilic surface (glass) one hydrophobic surface (A1-Teflon) and three super-hydrophobic surfaces (SHS-FAS, SHS-

Teflon and SHS-CNR1) whose characteristics are illustrated in Figure 2. A1-Teflon is a Teflon coated glasses (see [15] for more details). SHS-Teflon was fabricated on an aluminum substrate by aluminum etching in acid solution (to achieve the desired surface roughness) and subsequent spraying with Teflon[®] (10:1 v/v solution of FC-75 and Teflon[®] from DuPont[™]). SHS-FAS was fabricated by means of a one-step wet reaction, by treating an aluminum sample in a water solution of sodium hydroxide and perfluorooctyltriethoxysilane [16]. SHS-CNR1 was produced and supplied by ISTECH CNR (Italy) and is tested as received (no details on surface fabrication were provided due to pending patent).

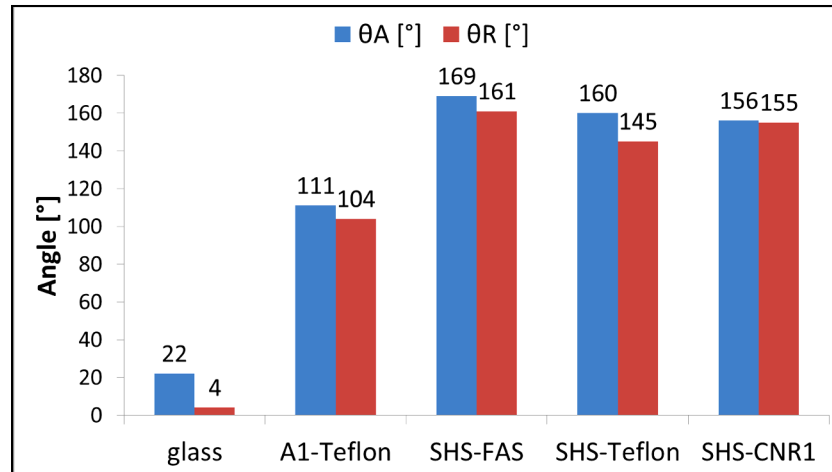


Fig 2. Advancing and receding contact angle of the tested surfaces.

The surface roughness can influence the impalement pressure and thus the rebound/sticking threshold. In Table 1 and Table 2 the roughness of the used surfaces is summarized.

Table 1. Surface roughness (RMS) of the hydrophobic surfaces. The reported value is the rms surface roughness, R_q , measured using Atomic Force Microscope MFP-3D (Asylum Research).

N	Surface	Roughness (RMS)
i	Glass	0.9 nm
ii	A1-Teflon	0.9 nm

Table 2. Surface roughness (R_a) of the super-hydrophobic surfaces. The reported values correspond to the mean surface roughness, R_a , measured using a roughness meter (Diavite DH-5, resolution 0.01 μm).

N	Surface	Roughness (R_a)
iii	SHS-FAS	1.03 μm
iv	SHS-Teflon	1.91 μm
v	SHS-CNR1	2.42 μm

3. EXPERIMENTAL APPARATUS

To accelerate the drop, an apparatus known as “Air Flow Accelerated Drop” (AFAD) is used. The layout of the experimental apparatus is illustrated in Fig 2a.

The drop generator (AFAD) is a convergent nozzle in which it is possible to create a drop and accelerate it to a target. Two stream flows (Figure 2b) are generated: primary and secondary stream. The primary stream flow is used in order to detach the drop with the desired in each experiment diameter, while the secondary stream flow accelerates the detached drop up to the desired impact velocity. The value of the stream flow is controlled by an ECU and by two proportional valves (primary and secondary stream flow) that can be operated up to 0.7 N/mm² inlet pressure, from complete close (0%) to full open (100%) positions.

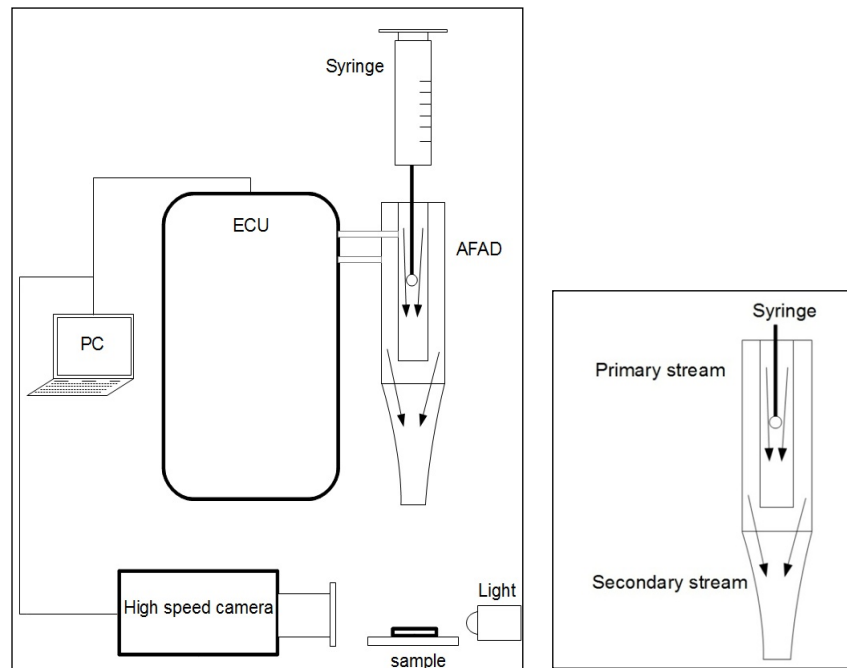


Fig 2. a) Apparatus for impact test with drop generator. **b)** Drop generator geometry with the air streams.

The drop impacts were recorded by a high speed camera (FASTCAM SA 1.1 - Photron©, the frame rate is set between 10000 and 100000 fps with a resolution of 256x256 pixel). Table 3 shows the impact parameters.

Table 3. Impact parameters for the Air Flow Accelerated Drop Generator.

Average drop velocity [m/s]	Drop diameter [mm]	Weber number
3-6	1-2	162-1111

The average drop impact velocity and the relative Weber number depend on the value of the stream flow (particularly on the value of the secondary stream) as well as on the diameter of the drop. The value of the impact velocity slightly varies at the same condition of the secondary air stream for different drop diameter. This is due to the deformation of the drop (which changes the drag force and then the drop acceleration) and the presence of turbulence in the stream flow. The impact velocity increases with the increase of the secondary stream flow rate. Due to their lower inertia the smallest drops can reach higher velocities when the secondary stream is low (0-70% of the maximum flow rate). In cases of high secondary stream flow rates (from 80% of the maximum flow rate) the impact velocity increases if the drop diameter increases, due to higher cross section area and hence a higher value of the drag force. The value of the average drop velocity is measured for each combination of secondary stream flow and drop diameter. Standard deviations for average drop velocities are ± 0.5 m/s.

4. EXPERIMENTAL RESULTS.

Five impact tests are performed aiming the following goals: 1) To evaluate the effect of the airflow on the maximum spreading (using an hydrophilic surface), by changing the distance between the surface and the nozzle, 2) To evaluate the drop impact morphology at high speed on surfaces with different wettability 3) To measure the rebound time on super-hydrophobic surfaces in order to estimate the influence of different impact velocities and different drop diameters, comparing the results with literature available correlations [14],[15] and finally 4) To investigate whether a Weber upper limit exists for drop rebound on hydrophobic and super-hydrophobic surfaces.

As mentioned previously, the primary air stream is used to detach the drop from the needle. In the present investigation its value is kept constant at 30% of its maximum allowed value (a lower value is not enough to detach the droplet, while a higher value may induce fragmentation of the drop). On the contrary, the secondary air stream, which controls the drop velocity changes between from 0% to 100% of its maximum allowable value.

Test 1: A preliminary test is carried on to find which distance between the generator and the surface does not influence the rebound time. In fact, if the drop is generated too close to the surface, the turbulence of the stream flow can strongly affect the measurement of the rebound time. In this test, for a fixed drop velocity (secondary stream value of 70%), the distance of the drop generator is varied into a range from 20 mm to 120 mm. Table 4 shows the test parameters for evaluating the effect of the airflow on the maximum spreading on a hydrophilic surface (glass).

Table 4. Experimental parameter for high-speed impact tests: effect of distance of the drop generator.

Surface	Secondary stream flow rate (%)	Droplet diameter (mm)	AFAD distance from the surface (mm)	Camera fps
Glass	70	1.42	20-40-60-80-100-120	10000

Test 2: In Table 5 the test parameters to study the effect of the impact velocity on super-hydrophobic surfaces are summarized. The tests are repeated for two different drop diameters, with 7 impact for each drop diameter and secondary stream flow. The time resolution of the high-speed camera is increased, using up to 30000 fps.

Table 5: Experimental parameters for high speed impact tests: effect of secondary stream flow rates.

Surface	Secondary stream flow rate (%)	Droplet diameter (mm)	AFAD distance from the surface (mm)	Camera fps
SHS-Teflon	0-30-60-70-80-100	0.98-1.42	100	30000
SHS-FAS	0-30-60-70-80-100	0.98-1.42	100	30000
SHS-CNR1	0-30-60-70-80-100	0.98-1.42	100	30000

Test 3: As mentioned previously, the drop diameter has an influence on the rebound time. The tests parameters for this test are summarized in Table 6. The test is performed for SHS-FAS, with 7 impact for each drop diameter and secondary stream flow.

Table 6. Parameters for high speed impact tests: effect of the drop diameter

Surface	Secondary stream flow (%)	Droplet diameter (mm)	AFAD distance from the surface (mm)	Camera fps
SHS-FAS	0	0.98-1.24-1.42-1.56-1.68-1.78	100	80000
SHS-FAS	80	0.98-1.24-1.42-1.56-1.68-1.78	100	80000
SHS-FAS	90	0.98-1.24-1.42-1.56-1.68-1.78	100	80000
SHS-FAS	100	0.98-1.24-1.42-1.56-1.68-1.78	100	80000

Test 4: A hydrophobic surface is tested with more than 20 impacts (Table 7) for different impact velocities in order to investigate if an upper limit of rebound exists. The main underlying assumption is that the probability of no rebound increases with the increase of the Weber number.

Table 7. Parameters for high speed impact test to find a statistical limit of no rebound

Surface	Secondary stream (%)	Droplet diameter (mm)	AFAD distance from the surface (mm)	Camera fps
A2	60-70-80-90-100	1.42	100	30000

4.1 Preliminary test: effect of airflow on the maximum spreading

For the first test, the distance of the drop generator from the surface is an experimental variable. If the drop generator is near the surface, the secondary stream value changes the air flow condition near the surface pushing the drop towards the sample. This increases the spreading of the drop, and hence the rebound time. It is necessary to find a distance which makes this effect negligible. Then this distance becomes a constant in the following tests. Some impacts on a hydrophilic surface (glass) are done, at the same impact velocity and drop diameter, but varying the distance of the drop generator. Then the diameter D_{\max} at the maximum spreading (the maximum diameter reached by the drop after the impact) is evaluated for different distances of the drop generator. The dimensionless maximum spreading ($D_{\max} / D_{\text{eq}}^1$) is depicted in Fig 3 as function of the distance of the drop generator from the surface. On glass no rebound occurs for any Weber number, and the drop impact creates a uniform thin film, due to the extremely low contact angle. In this shape (as a plate) it is very easy to measure the maximum spreading variation. As it can be observed for values greater than 100 mm, the influence of the distance on the maximum spreading is minor, since the difference between the value at 100 mm and 120 mm (5.06 and 4.90) is within the error bars. At these distances the effect of the air flow induced by the drop generator is probably small. The distance 100 mm is then kept constant in the following tests.

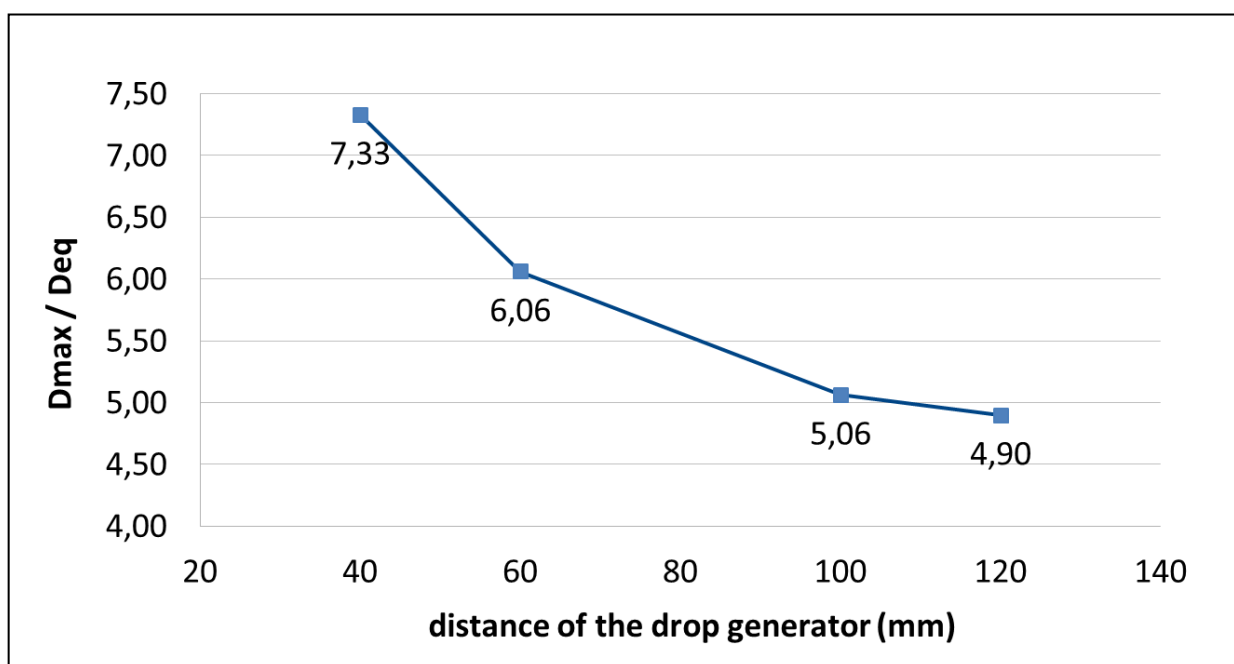


Fig 3. Maximum spreading as a function of the distance of the drop generator from the surface. The maximum spreading is normalized with the initial drop diameter D_{eq} ($D=1.42$ mm, secondary stream value = 70%, glass surface). Typical standard deviation is ± 0.5 m/s.

¹ D_{\max} is the drop maximum diameter after the impact (the maximum spreading) and D_{eq} is the diameter of the drop before impact.

4.2 Effect of impact velocity on the rebound time

The drop generator allows to perform drop impact experiments with relatively high impact velocity (up to 8 m/s). These tests show that the rebound time does not correlate with the impact velocity. Fig 4, depicts the results of the rebound time at different secondary stream values for the initial drop diameter ($D_{eq} = 0.98$ mm).

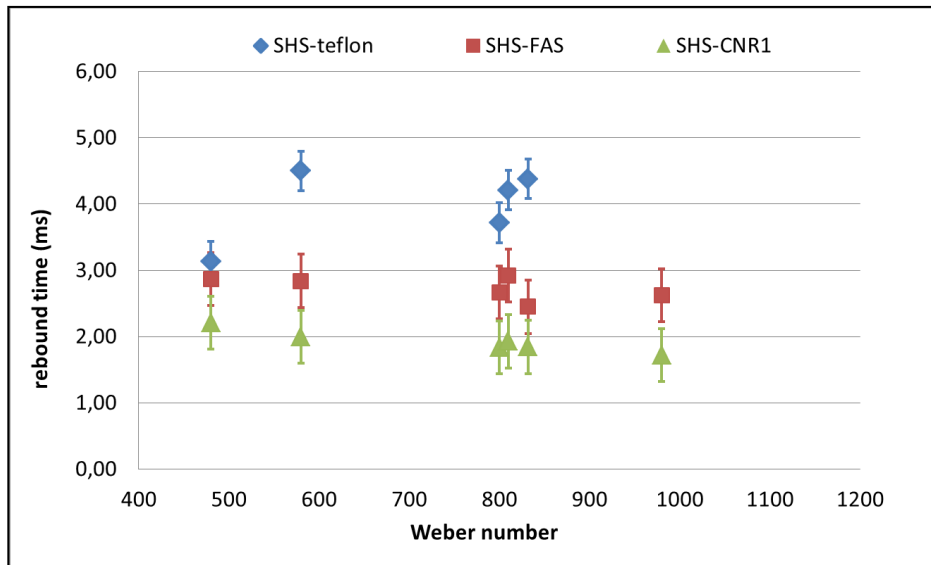


Fig 4. Drop rebound time for 3 super-hydrophobic surfaces (SHS-Teflon, SHS-FAS and SHS-CNR1) as function of the Weber number. Drop diameter is $0.98 \text{ mm} \pm 0.2 \text{ mm}$. Standard deviation is typically 2% of the mean value.

The rebound time is clearly constant, for all the surfaces in the whole range of the impact Weber number. Fig 5 compares the spread factor D_{max}/D_{eq} with two correlations reported in literature [13],[14]. The comparison shows a reasonable agreement with the present experimental data. Few points have a greater D_{max}/D_{eq} , probably due to the influence of the drop deformation before impact.

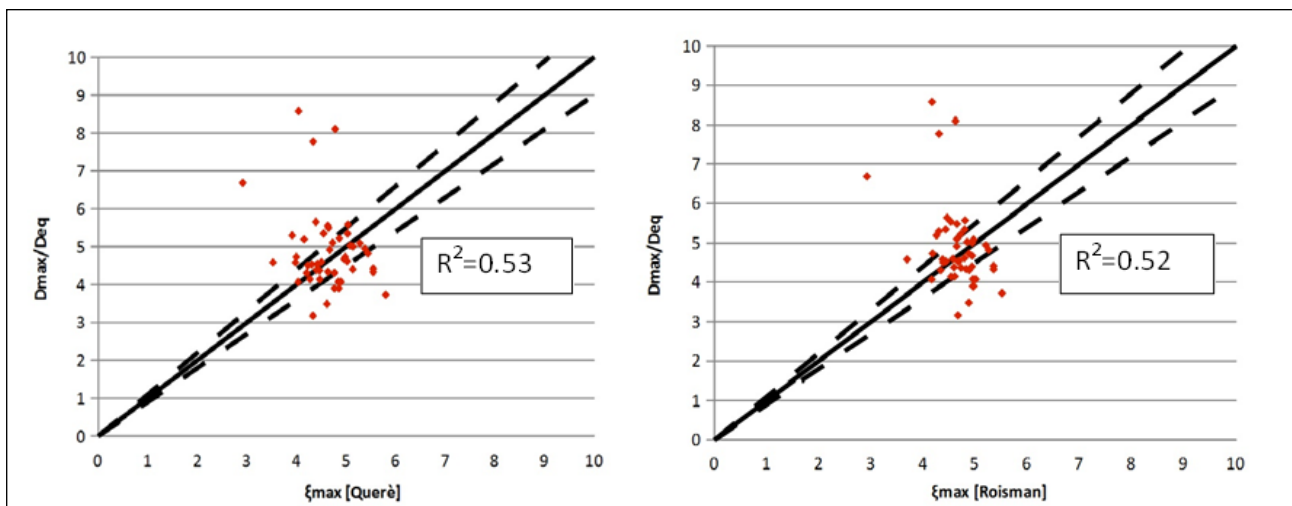


Fig 5. Comparison between the D_{max}/D_{eq} rate on SHS -Teflon evaluated in the experimental test with correlation [13] and [14]. R-squared is evaluated.

4.3 Effect of drop diameter on the rebound time

Figure 6 shows the influence of the drop diameter on the rebound time. The tests are repeated for 4 different secondary stream flow rates. The rebound time increases with the drop diameter increases, according to [18],

and for the same drop diameter the rebound time is not significantly influenced by the secondary stream flow rate. Again this result confirms that there is not a clear correlation between the velocity of the drop and the rebound time.

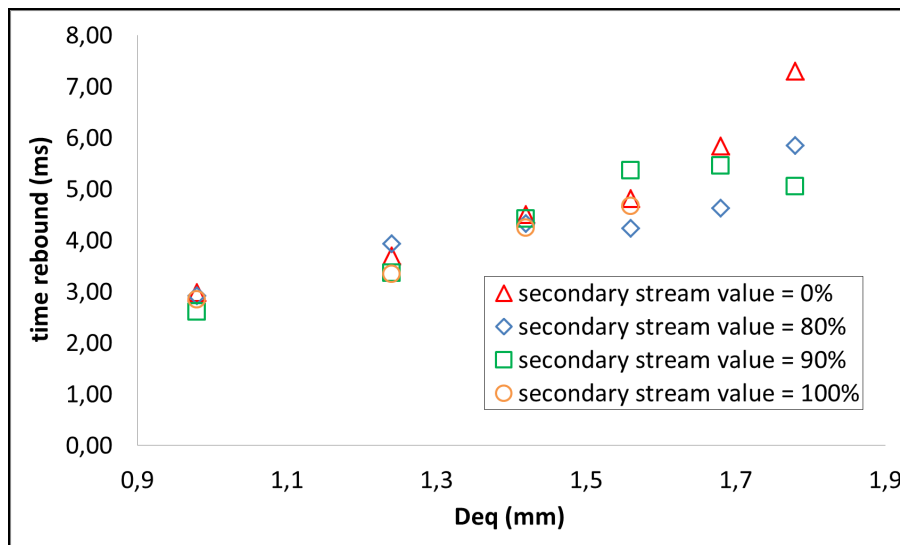


Fig 6. Drop rebound time on surface SHS-FAS as function of initial diameter of the drop (D_{eq}), at different secondary stream value).

Three different outcomes are illustrated in Fig 7, where the spatial and temporal evolution of the drop impact experiments is depicted for three different drop diameters. The morphology of the rebound doesn't change if the drop diameter increases. For all diameters a rapid spreading of the water breaks part of the drop into many small droplets with a high mobility. Instead, a central bulk of drop rebounds in a very short time.

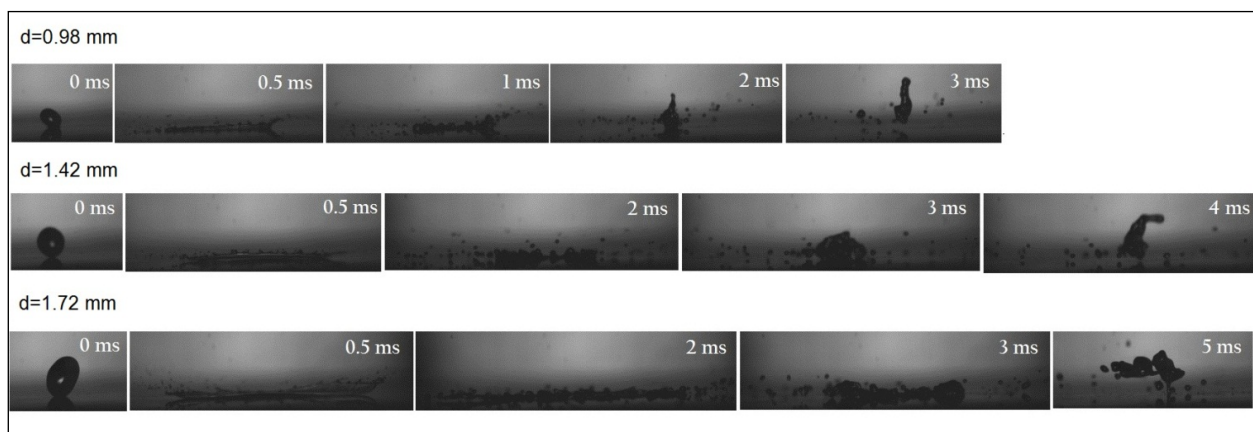


Fig 7. Water drop impacts on SHS-FAS for different drop diameter. The secondary stream value is 80%, camera fps is set to 80000 frame per second.

4.4 Upper limit of the Weber number for drop rebound

Finally experiments at different impact velocities with a fixed drop diameter are made on one hydrophobic surface (A2), to study whether the drop sticks to the substrate when the impact velocity increases. The idea is to use a statistical approach to model the rebound event. For low impact velocity values the rebound is always verified. When the impact velocity increases the probability of the rebound (number of rebounds compared to the amount of impacts) decreases. Two examples of rebound and no rebound situations are illustrated in Fig 8.

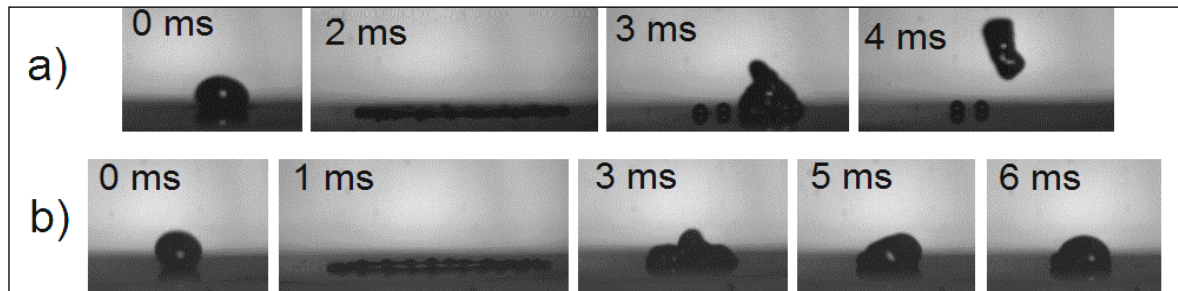


Fig 8. Example of rebound (a) and no rebound (b) of the drop on a hydrophobic surface A2. a) $We=854$, $D_{eq}=1.42$ mm, $fps=30000$ b) $We=1100$, $D_{eq}=1.42$ mm, $fps=30000$.

The statistical function, where there is the transition from rebound to no rebound, is evaluated by a large series of impact tests at a given Weber number. The number of rebounds compared to the total number of impacts is then evaluated. The results are showed in Fig 9. The probability density for the rebound is denoted $P(We)$.

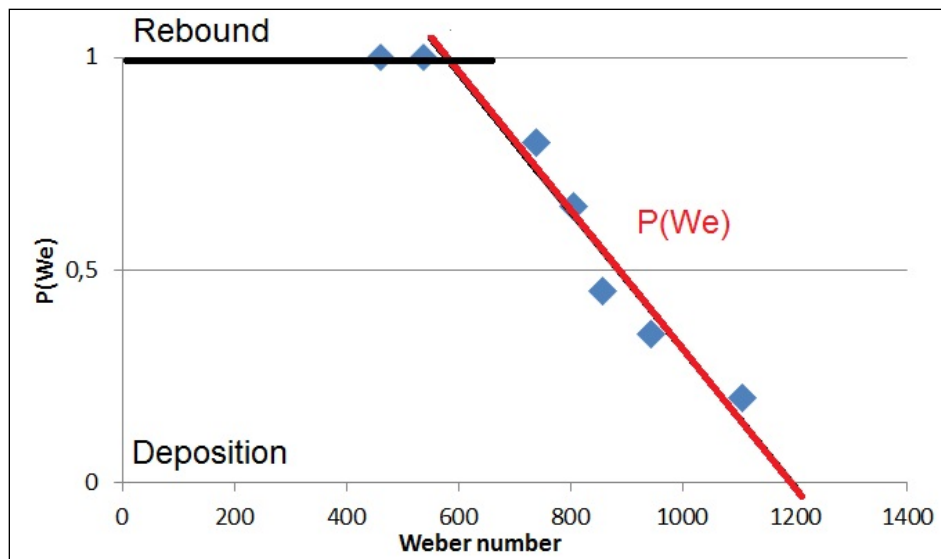


Fig 9. The probability density of rebound for A2 surface at different impact velocities. For an impact Weber number lower than 550, the rebound is certain on this surface (black line). The blue markers are the experimental results, correlated using the $P(We)$ function (red line).

The blue markers are the experimental results of the $P(We)$. For an impact Weber number lower than 550, the rebound is certain on this surface, so the value of P function in this velocity range is 1. The points with an impact Weber number greater than 550 are the results of this experimental study. All these points are correlated using this function:

$$P(We)=A+B(We)$$

A and B are the coefficients of the linear interpolation given in Table 8). Also some typical parameters are defined in Table 8: We_{max} is the maxim Weber number at which only the rebound was observed, and We_{cr} is the minimum Weber number at which the rebound has been never observed. Additionally the median value We_m is defined, corresponding to the probability density for rebound of 0.5.

Table 8. Rebound probability linear interpolation

Parameter	Value
A	1.916

B	-0.0016
R-square	0.91
We_{max} corresponding to $P = 1$	572
We_m corresponding to $P=0.5$	880
We_{cr} corresponding to $P=0$	1197

5 CONCLUSIONS

This present investigation is focused in studying the drop impact on hydrophobic and super-hydrophobic surfaces with a system, referred to as “*Air Flow Accelerated Drop (AFAD)*” generator. The drop is detached by a primary stream that allows creating the droplets, and a secondary stream accelerates the droplet into the nozzle. With this system it is possible to create small drops (because there is a stream which helps to detach them) and accelerate them over the limit of a typical gravity accelerated drop impact apparatus. Drop impacts on super-hydrophobic surfaces are studied in order to evaluate the effect of higher velocity impact (from 4 m/s to 8 m/s) on rebound time. It is confirmed that the rebound time is independent from the velocity of the impact. The average rebound times for the three SHS tested (SHS-Teflon, SHS-FAS and SHS-CNR1) are respectively 4 ms, 2.7 ms and 2 ms. The effect of different drop diameters was also studied. The rebound time increases when the drop diameter, in agreement with literature [18]. Finally, drop impacts for different velocities on hydrophobic surfaces are studied to find a condition of no rebound. If the velocity increases, the probability of the rebound (number of rebounds with respect to the number of impact tests) decreases. So it is possible to create a statistical function of rebound/no rebound. A rebound probability of 50% was found with a Weber number equal to 880 for the given surface roughness of the present surfaces. With these experiments it is possible to draw the rebound map, showed in Fig 10.

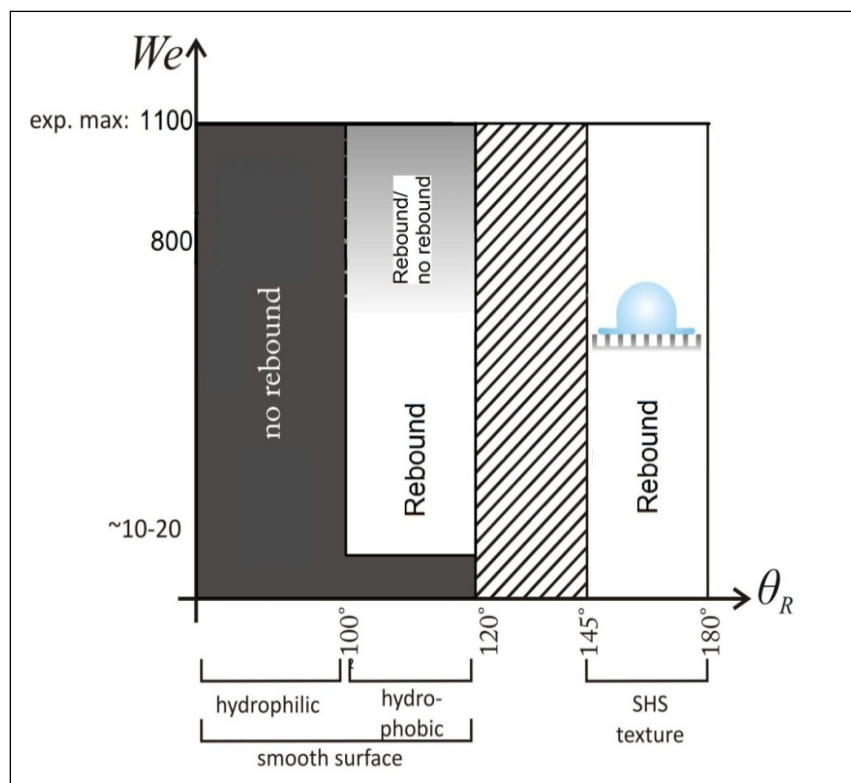


Fig 10. Rebound map for drop impacts onto dry surfaces

On hydrophilic surfaces ($\theta_r < 100^\circ$) rebound never occurs and the drop remains stuck on the surface for all Weber numbers. Rebound can be only observed for high receding contact angles. Data from a previous study

[10] indicate that drops do not rebound for $\theta_r \approx 90^\circ$, whereas they start rebounding on surfaces with $\theta_r \approx 105^\circ$. This is also confirmed by the present investigation at higher Weber numbers. As such, it is believed by the authors that $\theta_r \approx 100^\circ$ well represents the lowest boundary for drop rebound. For hydrophobic surfaces with higher contact angles ($100^\circ < \theta_r < 120^\circ$) the authors have previously observed [10] that there is a minimum limit for Weber number (in the range 10-20) under which rebound does not occur. The present investigation shows that also an upper limit exists: It is not a definite limit, but a statistical limit. The probability of no rebound, increases when the Weber number increases. For a Weber number of about 880, the probability of no rebound is 50%. With respect to SHS surfaces ($\theta_r > 135^\circ$), no lower limit was found, since drops rebound even when gently deposited. Also, tested SHS surfaces do not have any upper limit in the investigated range (up to $We = 1100$).

REFERENCES

- [1] Marengo, M., Antonini, C., Roisman, IV., Tropea, C., "Drop collisions with simple and complex surfaces". *Current Opinion in Colloid & Interface Science*, vol. 16, pp. 292-302, (2011). **Journal Paper**
- [2] Kannan, R., Sivakumar, D., "Impact of liquid drops on a rough surface comprising Microgrooves". *Exp Fluids*, vol. 44, pp. 927-938, (2008). **Journal Paper**
- [3] Rioboo, R., Tropea, C., Marengo, M., "Outcomes from a drop impact on solid surfaces". *Atom Sprays*, vol. 11, pp. 155-165, (2001). **Journal Paper**
- [4] Khranovskyy, V., Ekblad, T., Yakimova, R., Hultman, L., "Surface morphology effects on the light-controlled wettability of ZnO Nanostructures". *Applied Surface Science*, vol. 258, pp. 8146-8152, (2012). **Journal Paper**
- [5] Xu, L., "Liquid drop splashing on smooth, rough and textured surfaces". *PHYSICAL REVIEW E*, vol. 75, pp. 056-316, (2007). **Journal Paper**
- [6] Sikalo, S., Marengo, M., Tropea, C., Ganic, GN., "Analysis of impact of droplets on horizontal surfaces". *Exp Thermal Fluid Sci*, vol. 25, pp. 503-510, (2002). **Journal Paper**
- [7] Vander, RL., Berger, GM., Mozes, SD. "The combined influence of a rough surface and thin fluid film upon the splashing threshold and splash dynamics of a droplet impacting onto them". *Exp Fluids*, vol. 40, pp. 23-32, (2006). **Journal Paper**
- [8] Marmur, A., "Wetting on Hydrophobic Rough Surfaces: To Be Heterogeneous or Not To Be?". *Langmuir*, vol. 19, pp. 8343-8348, (2003). **Journal Paper**
- [9] Reyssat, M., Pépin, A., Marty, F., Chen, Y., Quéré, D., "Bouncing transitions on microtextured materials". *Europhys. Lett.*, vol. 74, pp. 306-312, (2006). **Journal Paper**
- [10] Antonini, C., Villa, F., Bernagozzi, I., Amirfazli, A., Marengo, M., (2013) "Drop Rebound after Impact: The Role of the Receding Contact Angle". *Langmuir*, 29 (52), pp 16045-16050, (2013). **Journal Paper**
- [11] Bartolo, D., Bouamrine, F., Verneuil, É., Buguin, A., Silberzan, P., Moulinet, S., "Bouncing or sticky droplets: Impalement transitions on super-hydrophobic micropatterned surfaces". *Europhys. Lett.*, vol 74, pp. 299-305, (2006). **Journal Paper**
- [12] Dhiman, R., Chandra, S., "Rupture of radially-spreading liquid films". *Phys. Fluids* vol. 20, pp. 092-104 (2008). **Journal Paper**
- [13] Roisman, IV., "Inertia dominated drop collisions. II. An analytical solution of the Navier-Stokes equations for a spreading viscous film". *Phys. Fluids*, vol. 21, pp. 052-104, (2009). **Journal Paper**
- [14] Clanet, C., Béguin, C., Richard, D., Quéré, D., (2004) "Maximal deformation of an impacting drop". *J. Fluid Mech* vol. 517, pp. 199-208, (2004). **Journal Paper**
- [15] Chen, H., Tang, T., Amirfazli, A., "Fabrication of Polymeric Surfaces with Similar Contact Angles but Dissimilar Contact Angle Hysteresis". *Colloid Surfaces A*, vol. 408, pp 17-21, (2012). **Journal Paper**
- [16] Bernagozzi I., Antonini C., Villa F., Marengo, M. "Fabricating super-hydrophobic aluminum: An optimized one-step wet synthesis using fluoroalkyl silane" submitted to Colloid Surface A. (2013). **Journal Paper**
- [17] Dhiman R., Chandra S., "Rupture of thin films formed during droplet impact". *Proc. R. Soc. A*, vol. 466, pp. 1229-1245, (2009). **Journal Paper**
- [18] D. Richard, C. Clanet, D. Quéré, "Contact time of a bouncing drop" *Nature*, vol 417, pp. 811, (2002). **Journal Paper**